Coherence properties of collective modes in ensembles of oscillators

Arkady Pikovsky [1,*] Franco Bagnoli [2,3,†] and Stefano Iubini [4,3,‡]

[1]*Department of Physics and Astronomy, University of Potsdam, Karl-Liebknecht-Str. 24/25, 14476, Potsdam-Golm, Germany*
[2]*Department of Physics and Astronomy and CSDC, University of Florence, via G. Sansone 1, I-50019, Sesto Fiorentino, Italy*
[3]*Istituto Nazionale di Fisica Nucleare, Sezione di Firenze, via G. Sansone 1, I-50019, Sesto Fiorentino, Italy*
[4]*Istituto dei Sistemi Complessi, Consiglio Nazionale delle Ricerche, via Madonna del Piano 10, I-50019, Sesto Fiorentino, Italy*

(Received 9 January 2026; accepted 22 April 2026; published 11 May 2026)

Synchronization transitions in oscillatory networks often manifest as the emergence of a periodic global mode. While perfect in the thermodynamic limit, this mode fluctuates for finite ensembles. We characterize the coherence of this mode in terms of the phase diffusion constant. In several examples, we always observed normal diffusion, but the dependence of the diffusion constant on the system size $D \sim N^{-\mu}$ depends on the nature of coupled units. For coupled chaotic systems, we found $\mu = 1$, while for coupled periodic oscillators we observed, depending on the particular model, values between 2 and 2.7. These large values of the power index are attributed to the size dependence of collective chaos in the finite ensemble, which disappears in the thermodynamic limit. We also show that in the standard Kuramoto model for a symmetric set of frequencies, there is an additional transition to a symmetric chaotic state with vanishing diffusion of the global phase.

DOI: 10.1103/lrp8-4wxh

I. INTRODUCTION

Clocks are not perfect: Due to ambient noise, the coherence time is finite. The phase of the periodic self-sustained oscillators diffuses due to noise, and the diffusion constant, which has the dimension of inverse time, determines the coherence time and the width of the spectral peak [1,2]. This concept can also be applied to collective oscillating modes appearing due to synchronization of individual units in large ensembles [3,4]. Such transitions are usually theoretically treated in the thermodynamic limit of an infinite number of units [5,6]. In this limit, the transition to synchrony appears as a transition from a steady mean field to an oscillating global mode (typically via a Hopf bifurcation [5,7,8]). A periodic regime in the thermodynamic limit has infinite coherence time (except for cases where the collective mode in the thermodynamic limit is chaotic [9–12]; we do not consider such regimes in this paper).

In experimental realizations of the synchronization transition, the number of interacting units N is necessarily finite, and in many cases rather small: 64 chemical oscillators in [13,14]; 72 electronic oscillators in [15]; 108 and 690 Josephson junctions in [16]; 40 photochemical oscillators in [17]; 1600 chemical Belousov-Zhabotinsky oscillators in [18]; several hundreds of lasers in [19]; 30 metronoms in [20]. In some cases, the number of interacting units is itself a bifurcation parameter. For example, the collective mode of the Millennium Bridge in London appeared when the number of walkers exceeded $N = 164$ [21].

For a finite number of coupled elements, the appearing global mode is subject to finite-size fluctuations (unless the full locking at a large coupling strength occurs). These fluctuations have been explored numerically and theoretically in [22–35]. However, in most cases, the focus was not on the coherence properties of the phase of the collective mode but on the finite-size effects in the amplitude dynamics. Only in Refs. [24,32] has the phase diffusion constant been demonstrated to scale $\sim N^{-1}$ with the population size for coupled noisy oscillators. Another situation in which the diffusion of the phase of the collective mode was studied is the Hamiltonian mean-field model [36,37]. There, due to momentum conservation, the dominant mode of motion of the collective phase is a ballistic one, with a transition to normal diffusion at a time that diverges with the system size.

The goal of this paper is to explore properties of the diffusion of the collective mode in ensembles of deterministic units. We demonstrate that coupled chaotic oscillators produce a regular mode with phase diffusion scaling $\sim N^{-1}$, like for coupled noisy units [24,32]. On the contrary, for ensembles of periodic oscillators, we observe a much stronger decay of the diffusion with the system size. We also describe a remarkable transition, due to symmetry, in the standard Kuramoto system to a fully phase-coherent (but still chaotic) regime with quenched diffusion.

Before proceeding to the consideration of particular systems, let us discuss the general conditions for the existence of the global phase. Suppose that in the thermodynamic limit, there is a Hopf-type transition from static to oscillating mean field at critical coupling ε_c. One usually characterizes the

*Contact author: pikovsky@uni-potsdam.de
†Contact author: franco.bagnoli@unifi.it
‡Contact author: stefano.iubini@cnr.it

transition with the amplitude of global oscillations R, which is zero for $\varepsilon < \varepsilon_c$ and is positive for $\varepsilon > \varepsilon_c$. Fluctuations due to finite-size effects smear the transition, so the amplitude R fluctuates and is nonzero at all couplings, and the average of R grows rapidly around ε_c. Still, as long as the amplitude of collective oscillations can vanish (or be very small) at some instants of time, the phase of these oscillations is ill-defined. Only when the amplitude R is distinct from zero is the phase well-defined. The criterion for the onset of the global oscillating mode based on finding the coupling strength ε_R beyond which $R_{\min} > \gamma$ for some small threshold γ, has been suggested and used in experiments [15,38] and numerically explored in [33]. Clearly, the existence threshold of the global collective mode ε_R depends on the system size and ε_R becomes closer to ε_c from above as $N \to \infty$; this threshold defines the domain with a well-defined phase where the phase diffusion properties can be explored.

II. KURAMOTO-SAKAGUCHI ENSEMBLE

Our first model is the Kuramoto-Sakaguchi (KS) system of globally coupled phase oscillators [39]:

$$\dot{\varphi}_k = \omega_k + \frac{\varepsilon}{N}\sum_{j=1}^{N}\sin(\varphi_j - \varphi_k - \alpha),\ k = 1,\dots N. \qquad (1)$$

The Kuramoto order parameter

$$Z(t) = N^{-1}\sum_k \exp[i\varphi_k(t)] = R(t)\exp[i\Theta(t)] \qquad (2)$$

can be considered as the complex amplitude of the collective mode, where R is the real amplitude and Θ is the phase of the collective global mode. We expect that for $\varepsilon > \varepsilon_R$, where the amplitude R is separated from zero, the phase Θ is well-defined, and one can calculate its averaged rotation velocity $\Omega = \lim_{T\to\infty} T^{-1}(\Theta(T) - \Theta(0))$, as well as the diffusion constant $D = \lim_{T\to\infty} T^{-1}\langle(\Theta(T) - \Theta(0) - \Omega T)^2\rangle$. The relevant parameter in problem (1) is the distribution of frequencies $g(\omega)$. In simple cases like Gaussian and Cauchy distributions (because of rotational invariance, one can set the center of the distribution at $\omega = 0$), transition to synchrony in the thermodynamic limit occurs via a Hopf bifurcation to a state with $R = \text{const}$ and $\Omega = \text{const}$.

In the simulation of a finite ensemble, one has to fix a way of choosing frequencies ω_k. We first consider a regular sampling [22,26,30,33,35] according to relation $\int_{-\infty}^{\omega_k} g(\xi)d\xi = (k - 1/2)/N$. This yields just one system for each N. In the first numerical example, we adopt for $g(\omega)$ a Gaussian distribution with unit variance. Figure 1 shows an example of the phase diffusion and the dependence of the diffusion constant D on the ensemble size N for parameters $\alpha = \pi/4$, $\varepsilon = 2.5$. The results show that with good accuracy, the power law $D \sim N^{-\mu}$ with $\mu \approx 2$ holds. This means that the diffusion constant decreases much more strongly with the system size than the variance of amplitude variations, which decreases in the supercritical regime as $\sim N^{-1}$ [22,31]. We attribute this strong drop of the diffusion constant to the presence of weak chaos, to be discussed below.

To see if the observed value of exponent μ is universal, we performed similar simulations for other distributions

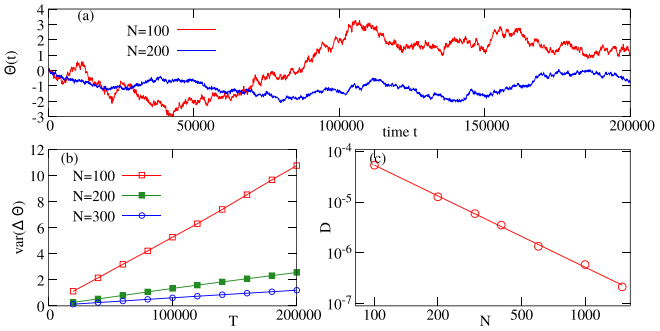

FIG. 1. (a) Examples of phase variations $\Theta(t) - \Omega t$ for $N = 100$, 200. (b) Examples of dependencies of the phase variance $\langle(\Theta(T) - \Theta(0) - \Omega T)^2\rangle$ vs time lag T; these dependencies are linear with high accuracy, indicating normal diffusion of the phase. (c) Log-log plot of the diffusion constants D vs N. The best fit has slope 2.01.

$g(\omega)$ of natural frequencies. In Fig. 2, we show phase diffusion constants for a Lorentz-Cauchy distribution $g(\omega) = (\pi(1 + \omega^2))^{-1}$ and for a uniform distribution $-1 \leqslant \omega \leqslant 1$. The exponents in these cases are different, but all of them are slightly larger than 2. In this figure, we also present the case of the Kuramoto ensemble ($\alpha = 0$) with a Gaussian distribution of natural frequencies, which demonstrates a larger exponent $\mu \approx 2.7$. The Kuramoto model demonstrates some special features of phase coherence, which we discuss below in Sec. V.

Above, we considered regular sampling, so, for each N, there is a unique system. If, in contrast, one uses random sampling, then for each N there is an ensemble of different systems with different values of the diffusion constant. To compare these constants at different N, we calculated the distribution functions of D at different N, using ≈1000 random samples for each N. Because the spread of diffusion constant at given N is large, we compare in Fig. 3 the distributions of $\log D$. The calculations are performed for the same parameters

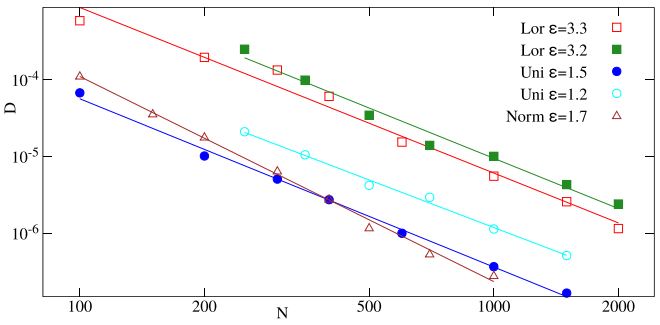

FIG. 2. Log-log plot of the diffusion constants D vs N different distributions of the natural frequencies and different parameters of the KS model (1). Open red squares: Lorentz-Cauchy distribution, $\varepsilon = 3.3$, $\alpha = \pi/4$, best fit $\mu = 2.16$. Filled green squares: Lorentz-Cauchy distribution, $\varepsilon = 3.2$, $\alpha = \pi/4$, best fit $\mu = 2.18$. Filled blue circles: Uniform distribution, $\varepsilon = 1.5$, $\alpha = \pi/4$, best fit $\mu = 2.19$. Open cyan circles: Uniform distribution, $\varepsilon = 1.2$, $\alpha = \pi/4$, best fit $\mu = 2.06$. Brown triangles: Gaussian distribution, $\varepsilon = 1.7$, $\alpha = 0$, best fit $\mu = 2.67$.

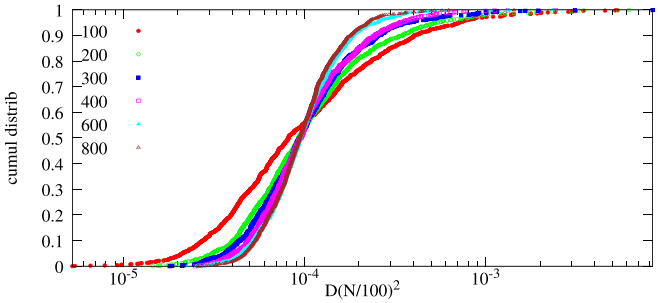

FIG. 3. Cumulative distributions of the diffusion constant D for different system sizes, plotted for rescaled quantity $D(N/100)^2$. Parameters are the same as in the case of regular sampling: $\varepsilon = 2.5$, $\alpha = \pi/4$.

as in Fig. 1. To check if the scaling $\sim N^{-\mu}$ with $\mu \approx 2$ holds, we depict the cumulative distributions of the rescaled diffusion constant $D(N/100)^2$ (so, for the smallest size $N = 100$, there is no rescaling). One can see that the plots intersect nearly at the same point at the level $1/2$, thus confirming the scaling $D \sim N^{-2}$.

III. OTHER EXAMPLES OF COLLECTIVE MODES IN ENSEMBLES OF CHAOTIC AND REGULAR UNITS

The KS is a representative example of a synchronization transition, but one cannot expect its quantitative properties to be universally valid. Here we present evaluations of the coherence of the global mode for three other models (their equations are given in the Appendix). The first model that exhibits qualitatively similar synchronization transition is the Morris-Lecar (ML) neuron model (A3). A single neuron is in spiking oscillatory states, and upon a strong enough coupling, a global periodic field appears in an ensemble. Some neurons with natural frequencies close to that of the mean field are locked, others are not entrained; this regime is similar to the synchronous state in the KS model (1). Calculations of the phase diffusion constant of the mean field reveal that it decays more strongly with the ensemble size: $D \sim N^{-2.48}$, see Fig. 4(b).

A regime where some oscillators are locked by the mean field while others are not is not the only type of synchrony in large ensembles. There exists so-called partial synchronization [40–43] where no one unit is locked, and nevertheless there is a collective oscillating mode; see [15,38] for an experimental observation in a set of electronic generators. As an example of such a type of synchrony, we use a globally nonlinear coupled system of SL oscillators (A2). For this model, the scaling of the diffusion constant with the system size is nearly the same as for the KS model above: $D \sim N^{-2}$, see Fig. 4(a) [best fits for different values of the distribution width of natural frequencies are in the range (1.92,2.03)].

Finally, we explored coherence properties of the collective mode for coupled chaotic oscillators. We took an ensemble of Roessler oscillators (A1). Each oscillator possesses a funnel attractor with ill-defined phase; however, the global mode is nearly periodic with well-defined phase, as shown in [44,45]. Diffusion constant in this case scales like $D \sim N^{-1}$, as shown in Fig. 4(c).

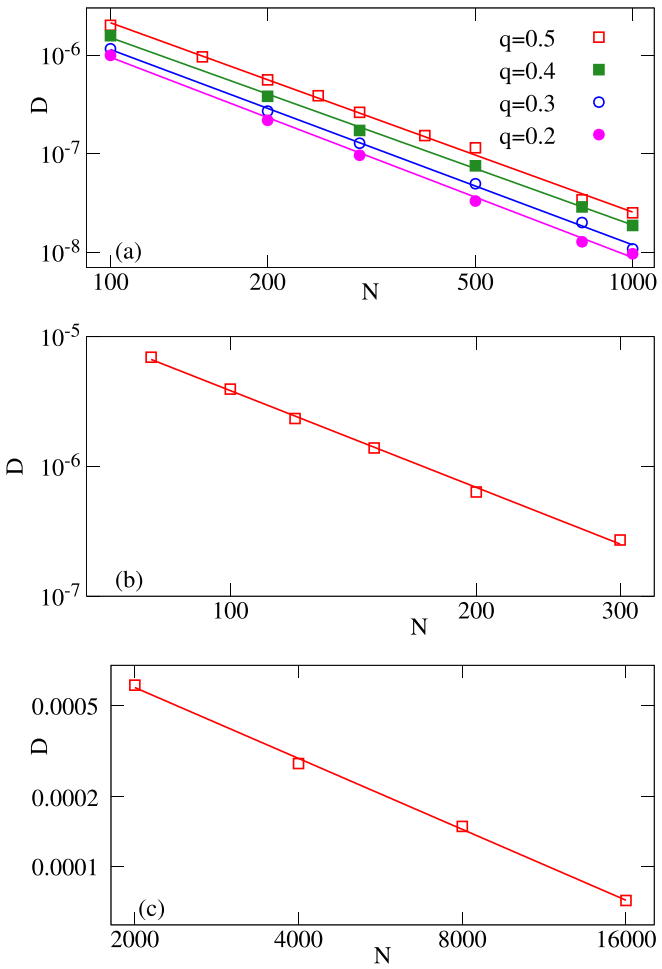

FIG. 4. System size dependencies (log-log plots) of the global phase diffusion constant for three models discussed in the text and formulated in the Appendix. (a) Nonlinearly coupled SL oscillators (A2) for four values of the frequency distribution half-width q. The best fit slopes are (from top to bottom) 1.92, 1.9, 1.98, 2.03. (b) Coupled ML system of neural spiking (A3). The slope of the best fit is 2.48. (c) Coupled chaotic Roessler systems (A1). The best fit slope is 1.02.

IV. COMPARISON TO SCALING OF THE LARGEST LYAPUNOV EXPONENT

We now explore why, in different cases, the diffusion constant of the global mode shows different dependencies on the system size. Let us introduce the instantaneous frequency of the global mode (global frequency) defined as $\Omega(t) = \dot{\Theta}(t)$. Because Θ is defined via mean fields, the process $\Omega(t)$ is also some kind of a mean field. For example, for the KS models (1) and (2), one has $\Omega = (NR)^{-1} \sum_k \cos(\varphi_k - \Theta)(\omega_k + \varepsilon R \sum(\Theta - \varphi_k - \alpha))$. We have found that in all considered examples the variance of the global frequency scales as $\mathrm{var}(\Omega) \sim N^{-1}$, see Fig. 5. However, it is not the variance of the stationary process $\Omega(t)$ that determines the diffusion constant, but, according to the Green-Kubo formula, the integral of the autocorrelation function (or, in spectral representation, the level of the continuous component of the spectrum at zero frequency). For the decay of the autocorrelation function, one needs the deterministic ensemble to be chaotic.

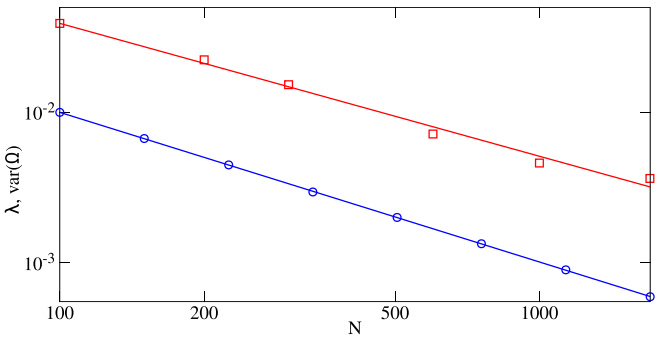

FIG. 5. System size dependencies of the variance of instantaneous frequency var(Ω) (blue circles, exponent 0.99) and of the largest Lyapunov exponent (red squares, exponent 0.89). The same parameters as in Fig. 1.

We have characterized this chaoticity by means of the largest Lyapunov exponent λ. For coupled chaotic Roessler systems, this exponent practically does not depend on the system size N, which explains why the diffusion constant in this case scales like $D \sim N^{-1}$, following the scaling of var(Ω).

In all other cases, the Lyapunov exponent tends to zero in the thermodynamic limit, as has been observed also for the Kuramoto model [46,47]. For the KS model (1) and for nonlinearly coupled SL oscillators (A2) we have found $\lambda \sim N^{-\nu}$ with ν close to 1 (see Fig. 5), while for the ML systems (A3) we have found $\lambda \sim N^{-0.56}$. This qualitatively explains why the diffusion constant decays strongly in these situations: in addition to a standard N^{-1} law for the variance of the global frequency, the chaotic component of its variations also vanishes in the thermodynamic limit. We stress here that the largest Lyapunov exponent is only indirectly related to the decay of correlations of the global frequency; in particular, the next example shows that in a chaotic ensemble, the diffusion constant can vanish identically.

V. SYMMETRY TRANSITION AND QUENCHED DIFFUSION IN THE KURAMOTO MODEL

Above we started with the KS model, not with the standard Kuramoto model [i.e., Eq. (1) with $\alpha = 0$]. The reason is that the latter demonstrates rather nontrivial properties of coherence. Next, we show that the Kuramoto model with a regular sampling of frequencies possesses a symmetric state in which phase diffusion is quenched, and this state is stable over a certain range of parameters. This symmetric state has been mentioned by Daido [22], without stability considerations, as a possible regime for corresponding symmetric initial conditions. Stability properties have been discussed in [46,48] and explored at small couplings in [49].

For definiteness, we assume the number of units $N = 2M$ to be even; for an odd N, a simple reformulation of the theory below is needed. We write the Kuramoto system as

$$\dot{\varphi}_k = \omega_k + \varepsilon(S\cos\varphi_k - C\sin\varphi_k), \quad C = \frac{1}{N}\sum_{j=1}^{N}\cos\varphi_j,$$

$$S = \frac{1}{N}\sum_{j=1}^{N}\sin\varphi_j \tag{3}$$

Furthermore, we assume that the frequencies are pairwise symmetric $\omega_k = -\omega_{-k}$. We introduce new variables

$$u_m = \frac{\varphi_m - \varphi_{-m}}{2}, \quad v_m = \frac{\varphi_m + \varphi_{-m}}{2}, \ m = 1, \ldots, M.$$

In these variables, the Kuramoto model (3) reads

$$\dot{u}_m = \omega_m - \varepsilon \sin u_m (C\cos v_m + S\sin v_m),$$

$$\dot{v}_m = \varepsilon \cos u_m (S\cos v_m - C\sin v_m),$$

$$C = M^{-1}\sum_{j=1}^{M}\cos u_j \cos v_j, \ S = M^{-1}\sum_{j=1}^{M}\cos u_j \sin v_j.$$

One can easily check that $v_1 = \ldots = v_M = V = \text{const}$ is the invariant manifold of this system of equations for arbitrary V. The arbitrariness of V reflects the invariance of the Kuramoto model with respect to a shift of all the phases. The complex mean field is represented through the introduced quantities as $Z(t) = R(t)e^{i\Theta(t)} = C(t) + iS(t)$, and the instantaneous global frequency is $\Omega(t) = \dot{\Theta} = (\dot{S}C - \dot{C}S)/(S^2 + C^2)$. On the other hand, on the symmetric manifold:

$$C = Q(t)\cos V, \quad S = Q(t)\sin V, \quad Q(t) = M^{-1}\sum_{j=1}^{M}\cos u_j.$$

Substituting these expressions in the instantaneous frequency of the global mode, we obtain that on the symmetric manifold $\dot{\Omega} = 0$. This means that the variations of the global frequency vanish and the diffusion is quenched. On the symmetric manifold, only the variables u_m vary, and in general their dynamics is chaotic. Existence of a symmetric manifold corresponds to the well-known effect of complete synchronization of chaotic systems [3,50,51].

According to the general theory of complete synchronization [3,52], stability of the chaotic symmetric state is determined by the largest transversal Lyapunov exponent on the symmetric manifold. To calculate it, we assume a weak violation of symmetry $v_m = V + w_m$, which, after linearization in w_m, leads to a system [where $u_m(t)$ is a chaotic trajectory on the symmetric manifold]

$$\dot{u}_m = \omega_m - \varepsilon \sin u_m \frac{1}{M}\sum_{j=1}^{M}\cos u_j, \tag{4}$$

$$\dot{w}_m = \varepsilon \cos u_m \frac{1}{M}\sum_{j=1}^{M}\cos u_m (w_j - w_m). \tag{5}$$

One can see from Eq. (5) that there is always a uniform solution $w_1 = \ldots = v_M$ with zero Lyapunov exponent; this solution corresponds to a shift of the constant V and it is not transversal. To calculate the transversal Lyapunov exponent, we thus set $\sum_j w_j = 0$.

We have calculated the transversal LE $\lambda_{tr} = \lim_{t\to\infty} t^{-1}\ln||w(t)||/||w(0)||$ for the Kuramoto model with regular sampled Gaussian distribution of frequencies for a range of system sizes. The results are presented in Fig. 6. The values of the transversal LEs vary significantly with the system size N, but the transition point ε_λ at which this exponent becomes negative only weakly depends on N, as is clear from Fig. 6(b), where the value of the coupling constant ε_λ at which the transversal Lyapunov exponent changes sign,

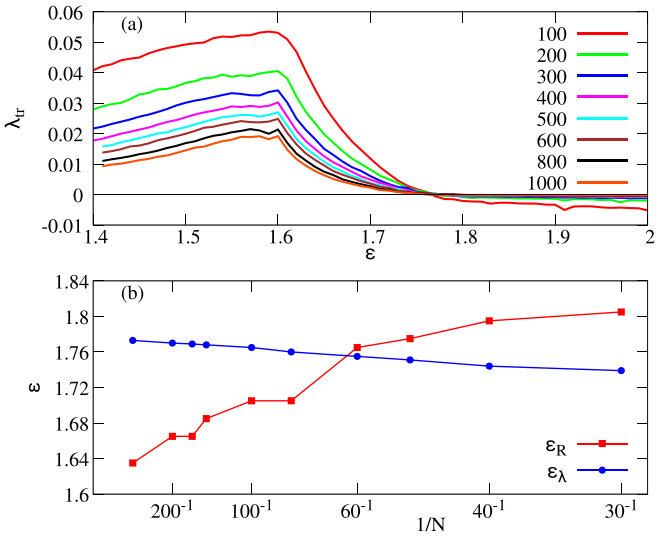

FIG. 6. (a) The transversal LE vs coupling parameter ε for several ensemble sizes N. (b) Blue circles show the critical value of coupling ε at which the transversal LE changes sign and the symmetric manifold becomes stable. Red squares: critical value of coupling at which a well-defined global mode with $R_{\min} > 0.1$ appears.

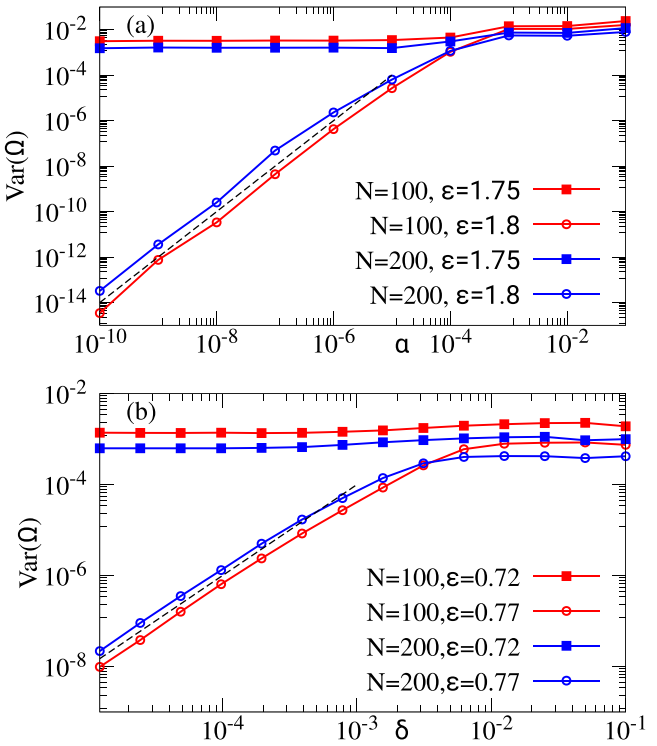

FIG. 7. (a) The variance of the global frequency vs. phase shift α in the KS system; for two values of coupling strength below and above the symmetry synchronization transition. (b) The variance of the global frequency vs asymmetry parameter δ of the beta distribution of frequencies in the Kuramoto model.

is presented. In this panel, we also show the value of the coupling ε_R, starting from which the minimal value of the order parameter R over a long run becomes larger than 0.1, which we use as an indicator for the existence of a global mode with a well-defined phase. One can see that the curves cross at $N_s \approx 60$. For smaller system sizes, the symmetric state becomes stable already in the state where the phase is ill-defined; thus, here, no regime with phase diffusion is observed. For $N > N_s$, there is a range of coupling constants $\varepsilon_R < \varepsilon < \varepsilon_\lambda$ where the phase is well-defined and diffuses (as illustrated in Fig. 2). With an increase of coupling strength, for $\varepsilon > \varepsilon_\lambda$, a symmetric state occurs with vanishing diffusion.

The symmetric state with vanishing global phase dynamics is destroyed if the symmetry of system (3) is broken. We illustrate this in Fig. 7 with two types of symmetry breaking. In the first example [Fig. 7(a)], we take the same symmetric natural frequencies as above, but insert a small phase shift α to the coupling terms, making the KS system out of the Kuramoto system. In the second example [Fig. 7(b)], we illustrate the situation where the coupling is symmetric, but the set of natural frequencies is slightly skewed. Namely, we sample these frequencies regularly from the beta distribution $B(3+\delta, 3-\delta)$ with a small skewness parameter δ. In both cases, the variance of the global frequency grows as the second power of the symmetry-breaking parameter.

VI. CONCLUSION

In this paper, we explored finite-size induced coherence properties of populations of coupled oscillators. The measure of coherence is the diffusion constant of the global mode's phase. The results provide a richer scenario, complementing previous studies of the amplitude fluctuations and of phase diffusion in an ensemble of noisy units. First, since the global phase is ill-defined prior to and in the vicinity of the synchronization transition; we used the condition that the global amplitude is separated from zero to define a region where calculation of the phase diffusion makes sense. Second, in this domain, we always observed normal diffusion, indicated by a linear growth of the variance of the phase differences as a function of the time lag. Third, we found that if the interacting units are chaotic, the diffusion scales as $D \sim N^{-1}$ with the same exponent as for coupled noisy units. The reason is that the effective disorder in the dynamics does not disappear in the thermodynamic limit, and the scaling is consistent with central-limit-theorem-like arguments. Fourth, for coupled periodic oscillators, we have found a much stronger decay of the diffusion constant with the system size, with powers ≈ 2 for the KS model and coupled SL oscillators, ≈ 2.5 for coupled ML neurons, and ≈ 2.7 for the Kuramoto model.

The values of the power appear to be rather sensitive to the parameters of the model and the distribution of natural frequencies. It is not clear if there are different universality classes; one needs to consider more examples. The strong decay of the diffusion constant can be attributed to weak system-size-dependent chaos in these models, characterized by the largest Lyapunov exponent that vanishes in the thermodynamic limit, which yields additional smallness to the usual $\sim N^{-1}$ decays of mean field fluctuations. In addition to the general features above, we have shown that the standard Kuramoto model with a symmetric set of natural frequencies exhibits, at sufficiently strong couplings, a symmetric state in which the global phase remains constant in time, although the

regime is chaotic. We expect this property to hold in other symmetric systems, such as coupled SL oscillators.

ACKNOWLEDGMENTS

S.I. acknowledges support from the MUR PRIN2022 project "Breakdown of ergodicity in classical and quantum many-body systems" (BECQuMB) Grant No. 20222BHC9Z. F.B. acknowledges support and hosting from the University of Perpignan via Domitia (France).

DATA AVAILABILITY

The data that support the findings of this article are not publicly available upon publication because it is not technically feasible and/or the cost of preparing, depositing, and hosting the data would be prohibitive within the terms of this research project. The data are available from the authors upon reasonable request.

APPENDIX: DYNAMICAL MODELS

Here we describe dynamical models of globally coupled oscillators used in the main text.

1. Coupled Roessler systems

This model has been studied in Refs. [44,45], it reads

$$\begin{aligned}\dot{x}_k &= -y_k - z_k + \frac{\varepsilon}{N}\sum_j x_j,\\ \dot{y}_k &= x_k + a y_k,\\ \dot{z}_k &= b + (x_k - c) z_k.\end{aligned} \tag{A1}$$

We use parameters $a = 0.25$, $b = 0.4$, $c = 8.5$, at which each Rössler system has a funnel-type attractor, i.e., the oscillators have an ill-defined phase. For this system, we use the observables

$$X(t) = \frac{1}{N}\sum_k x_k(t), \quad Y(t) = \frac{1}{N}\sum_k y_k(t).$$

The two-dimensional embedding is $(Y(t), X(t) + aY(t))$ because $\dot{Y} = X + aY$. These observables are normalized as $Y \to \frac{Y - \langle Y\rangle}{STD(Y)}$, and the same for $X + aY$, to obtain a maximally circular embedding. Then the phase of the mean field is calculated as arctan $\frac{Y}{X+aY}$. The diffusion constant vs N is presented in Fig. 4(c).

2. Coupled Stuart-Landau oscillators

This model has been studied in Ref. [53]. The equations read

$$\begin{aligned}\dot{a}_k &= (1 + i\omega_k)a_k - |a_k|^2 a_k + (\varepsilon_1 + i\varepsilon_2)A - \eta|A|^2 A,\\ A &= \frac{1}{N}\sum_k a_k.\end{aligned} \tag{A2}$$

Parameters are $\varepsilon_1 = \varepsilon_2 = 3$, $\eta = 10$. Note that the nonlinear mean field means many-body coupling (quadruplets) because $A|A|^2 = N^{-3}\sum_{jlm} a_j a_l a_m^*$. In Fig. 4(a), we show diffusion constants vs N for a uniform distribution of natural frequencies in an interval $(-q, q)$ for several values of q.

3. Coupled Morris-Lecar neurons

The ML model is a two-dimensional system describing spiking neurons. It is formulated in terms of variables (V, n), where V is voltage and $0 \leqslant n \leqslant 1$ is the portion of open potassium channels (the number of sodium channels m is taken from its equilibrium value m_∞ at a given voltage.) We adopt, following [54], the following model of N synaptically coupled ML systems ($k = 1, \ldots, N$; $\langle V\rangle = N^{-1}\sum_k V_k$):

$$\begin{aligned}\frac{dV_k}{dt} &= \frac{1}{C}\big(\varepsilon(\langle V\rangle - V_k) + I_{\mathrm{ext},k} - g_{Ca} m_{\infty,k}(V_k - V_{Ca})\\ &\quad - g_L(V_k - V_L) - g_K n_k(V_k - V_K)\big),\\ \frac{dn_k}{dt} &= (1 - n_k)\alpha(V_k) - n_k\beta(V_k).\\ m_{\infty,k} &= \frac{1}{2}\left(1 + \tanh\left(\frac{V_k - V_a}{V_b}\right)\right),\\ \alpha(V) &= \phi\frac{\cosh(\xi/2)}{1 + e^{-2\xi}}, \quad \beta(V) = \phi\frac{\cosh(\xi/2)}{1 + e^{2\xi}},\\ \xi &= \frac{V - V_c}{V_d}.\end{aligned} \tag{A3}$$

Inhomogeneity in the population is introduced by uniformly distributed external currents $100 \leqslant I_{\mathrm{ext},k} \leqslant 130$. Other parameters are $C = 20$; $V_K = -84$; $V_L = -60$; $V_{Ca} = 120$; $g_K = 8$; $g_L = 2$; $g_{Ca} = 4.4$; $V_c = 2$; $V_d = 30$; $\phi = 0.04$. A synchronized state where approximately half the oscillators are locked by the mean field is achieved at $\varepsilon = 0.28$, for this coupling the diffusion constants are shown in Fig. 4(b).

[1] I. Bershtein, On fluctuations close to a periodic motion of a self-oscillating system, DAN SSSR **20**, 11 (1938) (in Russian).

[2] E. Rubiola, *Phase Noise and Frequency Stability in Oscillators* (Cambridge University Press, Cambridge, 2008).

[3] A. Pikovsky, M. Rosenblum, and J. Kurths, *Synchronization. A Universal Concept in Nonlinear Sciences* (Cambridge University Press, Cambridge, 2001).

[4] J. A. Acebrón, L. L. Bonilla, C. J. P. Vicente, F. Ritort, and R. Spigler, The Kuramoto model: A simple paradigm for synchronization phenomena, Rev. Mod. Phys. **77**, 137 (2005).

[5] Y. Kuramoto, Self-entrainment of a population of coupled nonlinear oscillators, in *International Symposium on Mathematical Problems in Theoretical Physics*, edited by H. Araki Lecture Notes in Physics Vol. 39 (Springer, New York, 1975), p. 420.

[6] Y. Kuramoto, *Chemical Oscillations, Waves and Turbulence* (Springer, Berlin, 1984).

[7] E. Ott and T. M. Antonsen, Low dimensional behavior of large systems of globally coupled oscillators, Chaos **18**, 037113 (2008).

[8] H. Dietert, Stability and bifurcation for the Kuramoto model, J. Math. Pures Appl. **105**, 451 (2016).

[9] N. Nakagawa and Y. Kuramoto, From collective oscillations to collective chaos in a globally coupled oscillator system, Physica D **75**, 74 (1994).

[10] M.-L. Chabanol, V. Hakim, and W.-J. Rappel, Collective chaos and noise in the globally coupled complex Ginzburg-Landau equation, Physica D **103**, 273 (1997).

[11] P. Clusella and A. Politi, Between phase and amplitude oscillators, Phys. Rev. E **99**, 062201 (2019).

[12] P. Clusella and A. Politi, Irregular collective dynamics in a Kuramoto–Daido system, J. Phys.: Complexity **2**, 014002 (2021).

[13] I. Z. Kiss, Y. Zhai, and J. L. Hudson, Emerging coherence in a population of chemical oscillators, Science **296**, 1676 (2002).

[14] Y. Zhai, I. Z. Kiss, P. A. Tass, and J. L. Hudson, Desynchronization of coupled electrochemical oscillators with pulse stimulations, Phys. Rev. E **71**, 065202(R) (2005).

[15] A. A. Temirbayev, Y. D. Nalibayev, Z. Z. Zhanabaev, V. I. Ponomarenko, and M. Rosenblum, Autonomous and forced dynamics of oscillator ensembles with global nonlinear coupling: An experimental study, Phys. Rev. E **87**, 062917 (2013).

[16] P. Barbara, A. B. Cawthorne, S. V. Shitov, and C. J. Lobb, Stimulated emission and amplification in Josephson junction arrays, Phys. Rev. Lett. **82**, 1963 (1999).

[17] A. F. Taylor, P. Kapetanopoulos, B. J. Whitaker, R. Toth, L. Bull, and M. R. Tinsley, Clusters and switchers in globally coupled photochemical oscillators, Phys. Rev. Lett. **100**, 214101 (2008).

[18] J. F. Totz, J. Rode, M. R. Tinsley, K. Showalter, and H. Engel, Spiral wave chimera states in large populations of coupled chemical oscillators, Nat. Phys. **14**, 282 (2018).

[19] S. Mahler, A. A. Friesem, and N. Davidson, Experimental demonstration of crowd synchrony and first-order transition with lasers, Phys. Rev. Res. **2**, 043220 (2020).

[20] E. A. Martens, S. Thutupalli, A. Fourriere, and O. Hallatschek, Chimera states in mechanical oscillator networks, Proc. Natl. Acad. Sci. USA **110**, 10563 (2013).

[21] P. Dallard, T. Fitzpatrick, A. Flint, A. Low, R. R. Smith, M. Willford, and M. Roche, London Millennium Bridge: Pedestrian-induced lateral vibration, J. Bridge Eng. **6**, 412 (2001).

[22] H. Daido, Scaling behaviour at the onset of mutual entrainment in a population of interacting oscillators, J. Phys. A: Math. Gen. **20**, L629 (1987).

[23] H. Daido, Intrinsic fluctuations and a phase transition in a class of large populations of interacting oscillators, J. Stat. Phys. **60**, 753 (1990).

[24] A. Pikovsky and S. Ruffo, Finite-size effects in a population of interacting oscillators, Phys. Rev. E **59**, 1633 (1999).

[25] H. Hong, H. Park, and M. Y. Choi, Collective synchronization in spatially extended systems of coupled oscillators with random frequencies, Phys. Rev. E **72**, 036217 (2005).

[26] H. Hong, H. Chaté, H. Park, and L.-H. Tang, Entrainment transition in populations of random frequency oscillators, Phys. Rev. Lett. **99**, 184101 (2007).

[27] E. J. Hildebrand, M. A. Buice, and C. C. Chow, Kinetic theory of coupled oscillators, Phys. Rev. Lett. **98**, 054101 (2007).

[28] M. A. Buice and C. C. Chow, Correlations, fluctuations, and stability of a finite-size network of coupled oscillators, Phys. Rev. E **76**, 031118 (2007).

[29] L.-H. Tang, To synchronize or not to synchronize, that is the question: Finite-size scaling and fluctuation effects in the Kuramoto model, J. Stat. Mech.: Theory Exp. (2011) P01034.

[30] I. Nishikawa, K. Iwayama, G. Tanaka, T. Horita, and K. Aihara, Finite-size scaling in globally coupled phase oscillators with a general coupling scheme, Prog. Theor. Exp. Phys. **2014**, 23A07 (2014).

[31] H. Hong, H. Chaté, L.-H. Tang, and H. Park, Finite-size scaling, dynamic fluctuations, and hyperscaling relation in the Kuramoto model, Phys. Rev. E **92**, 022122 (2015).

[32] G. A. Gottwald, Finite-size effects in a stochastic Kuramoto model, Chaos **27**, 101103 (2017).

[33] F. Peter and A. Pikovsky, Transition to collective oscillations in finite Kuramoto ensembles, Phys. Rev. E **97**, 032310 (2018).

[34] A. Suman and S. Jalan, Finite-size effect in Kuramoto oscillators with higher-order interactions, Chaos **34**, 101101 (2024).

[35] O. E. Omel'chenko and G. A. Gottwald, Mean-field approach to finite-size fluctuations in the Kuramoto-Sakaguchi model, arXiv:2511.03700.

[36] F. Ginelli, K. A. Takeuchi, H. Chaté, A. Politi, and A. Torcini, Chaos in the Hamiltonian mean-field model, Phys. Rev. E **84**, 066211 (2011).

[37] T. M. Rocha Filho and B. Marcos, Classical Goldstone modes in long-range interacting systems, Phys. Rev. E **102**, 032122 (2020).

[38] A. A. Temirbayev, Z. Z. Zhanabaev, S. B. Tarasov, V. I. Ponomarenko, and M. Rosenblum, Experiments on oscillator ensembles with global nonlinear coupling, Phys. Rev. E **85**, 015204(R) (2012).

[39] H. Sakaguchi and Y. Kuramoto, A soluble active rotator model showing phase transition via mutual entrainment, Prog. Theor. Phys. **76**, 576 (1986).

[40] C. van Vreeswijk, Partial synchronization in populations of pulse-coupled oscillators, Phys. Rev. E **54**, 5522 (1996).

[41] P. Mohanty and A. Politi, A new approach to partial synchronization in globally coupled rotators, J. Phys. A: Math. Gen. **39**, L415 (2006).

[42] M. Rosenblum and A. Pikovsky, Self-organized quasiperiodicity in oscillator ensembles with global nonlinear coupling, Phys. Rev. Lett. **98**, 064101 (2007).

[43] A. Pikovsky and M. Rosenblum, Self-organized partially synchronous dynamics in populations of nonlinearly coupled oscillators, Physica D **238**, 27 (2009).

[44] A. Pikovsky, M. Rosenblum, and J. Kurths, Synchronization in a population of globally coupled chaotic oscillators, Europhys. Lett. **34**, 165 (1996).

[45] A. Pikovsky and M. Rosenblum, A unified quantification of synchrony in globally coupled populations with the Wiener order parameter, Chaos **34**, 053109 (2024).

[46] O. V. Popovych, Y. L. Maistrenko, and P. A. Tass, Phase chaos in coupled oscillators, Phys. Rev. E **71**, 065201(R) (2005).

[47] M. Carlu, F. Ginelli, and A. Politi, Origin and scaling of chaos in weakly coupled phase oscillators, Phys. Rev. E **97**, 012203 (2018).

[48] Y. L. Maistrenko, O. Popovych, and P. Tass, Desynchronization and chaos in the Kuramoto model, in *Dynamics of Coupled Map Lattices and of Related Spatially Extended Systems*, Lecture Notes in Physics Vol. 671 (Springer, Berlin, Heidelberg, 2005), pp. 285–306.

[49] H. Chiba and D. Pazó, Stability of an [*N*/2]-dimensional invariant torus in the Kuramoto model at small coupling, Physica D **238**, 1068 (2009).

[50] H. Fujisaka and T. Yamada, Stability theory of synchronized motion in coupled-oscillator systems, Prog. Theor. Phys. **69**, 32 (1983).

[51] A. S. Pikovsky, On the interaction of strange attractors, Z. Phys. B **55**, 149 (1984).

[52] A. Pikovsky and A. Politi, *Lyapunov Exponents. A Tool to Explore Complex Dynamics* (Cambridge University Press, Cambridge, 2016).

[53] M. Rosenblum and A. Pikovsky, Two types of quasiperiodic partial synchrony in oscillator ensembles, Phys. Rev. E **92**, 012919 (2015).

[54] G. Tanaka, K. Morino, H. Daido, and K. Aihara, Dynamical robustness of coupled heterogeneous oscillators, Phys. Rev. E **89**, 052906 (2014).